České Vysoké Učení Technické v Praze
Fakulta Elektrotechnická

Czech Technical University in Prague
Faculty of Electrical Engineering

Ing. Radek Procházka, Ph.D.

Dynamické modely pro predikci výsledků impulzních vysokonapěťových testů při znečištění a námraze

Dynamic models for the impulse voltage test results prediction under the ice and pollution conditions

Summary

The majority of insulation systems is exposed to outdoor conditions such as pollution, rain, snow, ice or fog and their combination as well. These external influences can significantly reduce the electrical strength and consequently cause the outage of electricity supply. The research activities in the field of experimental investigation of insulator flashover performance under such adverse conditions are very costly. Usually, the large climatic rooms are needed to simulate such conditions. The using of mathematical simulation models for flashover voltage predictions seems to be a good idea how to reduce costs. On the other hand, the simulation models requires deep knowledge of both physical processes of streamers and leader propagation and dynamic calculation of electric field distribution. The proposal of dynamic mathematical model and its experimental validation for a suspension insulator string, which is exposed to the transient overvoltage, is the main objectives of this lecture.

Souhrn

Větší část izolačních systémů je vystavena působení venkovních podmínek jako je znečištění, déšť, sníh, led nebo mlha a také jejich kombinaci. Tyto externí vlivy mohou výrazně redukovat elektrickou pevnost a následně zapříčinit výpadek dodávky elektrické energie. Výzkumné aktivity založené na experimentálním vyšetřování elektrické pevnosti, za takto nepříznivých podmínek, jsou často velmi nákladné, protože obvykle probíhají v klimatických komorách. Využití matematických simulačních modelů pro predikci přeskokových napětí je tak vhodný způsob, jak snížit celkové náklady. Na druhou stranu, použití simulačních modelů vyžaduje hlubokou znalost jak fyzikálních procesů šíření striméru a lídru, tak dynamického výpočtu rozložení elektrického pole. Návrh dynamického matematického modelu a jeho experimentální ověření pro závěsný izolátorový řetězec, který je vystaven působení přechodného přepětí, je hlavním cílem této přednášky.

Klíčová slova

Vysokonapěťové zkoušky, znečištění, námraza, přechodná přepětí, matematické simulace

Key words

High voltage tests, pollution, icing, transient overvoltage, mathematical simulation

Contents

1 Introduction **5**

2 Streamer - Leader formation and propagation **5**

3 Dynamic numerical model of discharge propagation on insulator string **11**
3.1 Simulation process proposal 11
3.2 Electric field calculation 13

4 Experimental verification of numerical model **19**
4.1 Experimental setup 19
4.2 Ice formation and the test procedure 20
4.3 Experimental results 22
4.4 Influence of ice thickness on the insulator flashover voltage 22
4.5 Simulation results and verification 24

5 Conclusion **24**

6 Ing. Radek Prochazka, Ph.D. **29**

1 Introduction

The high voltage tests and measuring techniques belong among traditional parts of electric power system. The gradually growing demand for electrical energy causes increasing of transmission voltages. In recent decades, the rapidly increasing of transmission voltages can be observed as a consequence of the development of large electric power stations far from centers of industrial production. At the same time, as the present cost of power electronic elements is reduced, the application of high-voltage direct current transmission, flexible ac transmission systems or static synchronous compensators is incre asing. It has been found that some high voltage equipments causes very fast front transients that may damage the insulation system. The majority of insulation systems are exposed to the influence of weather conditions as pollution, rain, snow, ice or fog. Weather conditions may change rapidly and unpredictably. Moreover, the speed of these changes is still increasing. The sudden appearance of ice and snow is also observed in areas that are not in traditionally cold regions. It has been proved that the presence of ice on insulators may lead to the insulator flashover and consequent power outage. The influence of atmospheric icing on insulator flashover performance is usually studied experimentally in large climatic rooms. These tests are very costly and time-consuming. So the simulation models for preliminary prediction of flashover voltages are needed. The proposed dynamic simulation model allows to calculate flashover voltages for different shapes of impulse voltages and to take into consideration an influence of pollution and icing conditions.

2 Streamer - Leader formation and propagation

The physical and experimental background of streamer-leader propagation for a long air gap was intensively studied by many investigators in the eighties and nineties of the last century [1–6]. It was found that the discharge development consists of several phases, which are described in the Fig.1.

At the beginning, when the applied voltage is increasing, the

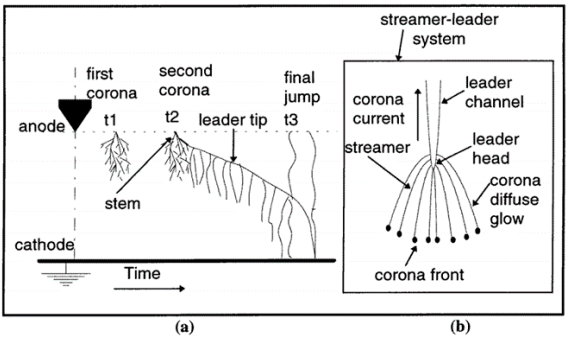

Figure 1: Streamer - leader process for long gap configuration [7]

discharge process is initiated by the formation of the first corona which is usually described as a luminous branched filaments - streamers. The criterion for streamer development is given by the critical gain 10^8 of ions at the head of an avalanche. The condition for streamer inception and propagation can be formulated as:

$$e^{\int_0^{x_s} (\alpha \quad \eta) dx} > N_{stab}, \tag{1}$$

where x_s is the length of streamer, α is the ionization coefficient, η is ion attachment coefficient, and N_{stab} is a minimum of charge at which the streamer is stable. The distribution of the ion charge along the streamer path, as a result of the simulation model, is shown in Fig. 2. It can be seen, that the number of ions is increasing in the high field region up to the maximum and then decreasing until the streamer propagation stops. The maximum is reached at applied field approximately 6.8 kV/cm.

Bondiou and Gallimberti introduced in [8] a model for the calculation of the number of positive ions in the streamer head as:

$$N(x) = \frac{2eR + \mu}{4a}(V_0 + \frac{4a}{2eR + \mu} N_0 \quad \frac{\beta}{2eR + \mu} x \quad V(x)), \tag{2}$$

where R is the radius of streamer head, V_0 is the potential in

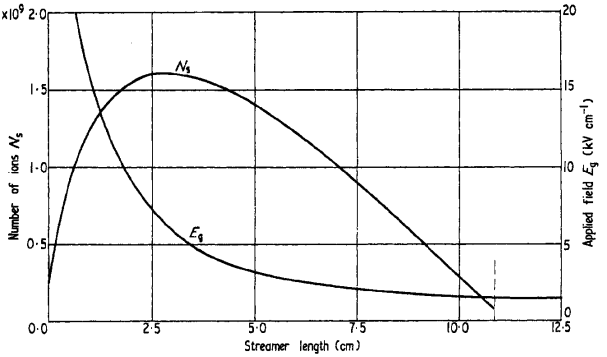

Figure 2: Distribution of the number of positive ions and applied field along the streamer (150 cm gap, 123 kV inception voltage) [1]

$x = 0$, N_0 is the number of positive ions in $x = 0$, $V(x)$ is the potential distribution along x-direction and $a = \frac{0.4e^2}{4\pi\epsilon_0}$. Coefficients μ and β represents loss and gain of energy, e is elementary charge and ϵ_0 is vaccum permitivity.
The streamer stability condition is then expressed as:

$$E(x) = \frac{\beta}{2eR + \mu}. \tag{3}$$

As can be seen from equation (3) the stability condition of streamer propagation depends on the coefficients β and μ and the streamer head radius R. The authors determined the stability field values for both polarities $E_{s+} \approx 500\ kV/m$ and $E_s \approx 750\ kV/m$ which is consistent with the experimental observations. These values can be used for simplified calculations of the streamer extension. The streamer length is directly given by the geometrical arrangement, if the constant stability field along the streamer extension is assumed. The total streamer space charge is calculated using equation:

$$\Delta Q = 4\pi k\epsilon_0 \int_0^{x_s} u(t_1, x) \quad u(t_2, x)dx, \tag{4}$$

where k is a geometric factor and $u(t_1, x) \quad u(t_2, x)$ expresses the

potential change in the streamer region. The streamer is transformed to the leader channel when the total space charge in the streamer region reaches the value of approximately 1 μC [9] . The simplified model for k factor calculation can be found in the appendix of [7]. The N parallel streamer filaments with the length l are assumed in this model. The distance of filaments from the central filament is assigned as a_i and the same charge distribution along a streamer filaments is supposed. Then the k factor can be expressed as:

$$k = \frac{N}{ln(\frac{l+\sqrt{l^2+a^2}}{a}) + \sum_{i=1}^{N-1} ln(\frac{l+\sqrt{l^2+a_i^2}}{a_i})}. \tag{5}$$

For the short distances, streamer can directly bridge the gap between electrodes and after that the flashover occurs. In case of longer gaps the leader propagation phenomena will starts.

The new structure called leader is created after the streamer channel is established. This transition is accompanied by a temperature increasing from approximately 300 K to 1000-1200 K. This energy gain leads to the many effects which drastically increase the conductivity of the stem and the electric field at its tip. The higher electric field generates the second streamer corona and the leader advancement process. The leader channel is formed as a thin luminous channel, connecting the corona zone to the high voltage electrode. The leader channel diameter (0.5 - 1 mm for 1.5 m gap) depends on the total charge flowed through the leader. The injected current induces the Joule heating of the gas in front of the leader's head and the conductivity increases. The leader's head is moving towards the opposite electrode when the axial velocity has a random fluctuation. The effective value of velocity v_l is proportional to the current I_l

$$v_l = \frac{I_l}{q_l}, \tag{6}$$

when the constant q_l represents the charge needed for a unit length leader advancement. The required charge depends on many factors. The measured and theoretically calculated dependency of q_l

on absolute humidity for different impulse durations is shown in Fig. 3.

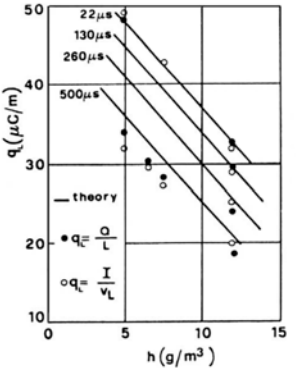

Figure 3: Calculated and experimentally measured values of charge per unit length as absolute humidity dependance for different impulse front times) [10]

As can be seen the q_l achieves the values from 20 $\mu s/cm$ to 50 $\mu s/cm$ within the relative humidity 30-70 % at normal pressure and temperature. The more detailed theoretical derivations and formulas were published in [10].

Described processes expand the channel and modify the internal electric field. As the leader approaches the final jump, the electric field distortion due to the leader space charge starts to play a decisive role. The different equations and numerical models have been introduced to simulate the leader channel inception voltage and advancement. Mathematical models based on the physical description have been mainly validated by experimental measurements of Les Renardieres' Group. A model presented by Rizk [11–13] is often used for engineering simulations as more practical and representative. This model provides expression of continuous leader inception voltage and breakdown voltage for different rod-plane gaps. The Rizk's expression for continuous leader inception voltage has a form of:

$$V_{lc} = \frac{V_{c\infty}}{1 + \frac{A}{R}}, \tag{7}$$

where $V_{c\infty}$ and A are constants respecting different values for rod-type and conductor-type gaps and R is a function of electrode configuration and the gap distance d. Besides the continuous leader inception voltage V_{lc} the leader voltage drop ΔV_l has to be expressed. The Rizk's formula for leader voltage drop is based on the assumption that the leader conductance per unit length G is given by Hochrainer's dynamic equation, which for the constant current leader propagation has a form:

$$G(t) = G_\infty + (G_i - G_\infty)e^{\frac{-t}{\theta}}, \tag{8}$$

where t is the lifetime of the leader section, G_i and G_∞ are the initial and ultimate values and θ is a time constant.

Assuming the constant speed of leader propagation and the leader gradient E_l is related to the conductance per unit length G and the leader current I_l by

$$E_l = \frac{I_l}{G}, \tag{9}$$

the proposed final formula for the leader voltage drop can be written as:

$$\Delta V_l = l_z E_\infty + x_0 E_\infty \ln\left(\frac{E_i}{E_\infty} - \frac{E_i - E_\infty}{E_\infty} e^{\frac{-l_z}{x_0}}\right), \tag{10}$$

where E_i and E_∞ are the initial and ultimate leader gradient, l_z is the axial leader length and $x_0 = v_l\theta$.

The final stage of the leader propagation - final jump - occurs when the streamer zone reach the opposite electrode. As the streamer zone becomes shorter, its average field increases. It leads to the higher leader velocity as high as 10^9 cm/s at $E \approx 20$ kV/cm [14].

3 Dynamic numerical model of discharge propagation on insulator string

The proposed numerical model is based on the physical streamer-leader process in long air gaps presented by many authors in various modifications. A complete mathematical description of this physical process is very difficult and some parts even still remain unclear. This is the reason why researchers usually work with simplified mathematical equations to find optimal model regarding purposes of simulations. Generally, the more often used streamer-leader models are coupled with a calculation of the electric field distribution and streamer-leader propagation. The electric field distribution can be in some cases (e.g. rod-plate gaps) expressed by analytical formulas, however nowadays the numerical FEM calculations are more frequent. The streamer-leader initiation and propagation model is usually partly based on experimentally determined characteristics and parameters. The physical background of the stremer-leader flashover process with assumptions and constrains for mathematical simulations was described in the previous chapter. The following describes the simulation model for the prediction of flashover voltage of suspension insulator string during the impulse high voltage testing under the pollution and ice condition. The proposed model was built up for the purposes of experimental results validation and also as a tool for the flashover voltage prediction.

3.1 Simulation process proposal

A flow chart of the proposed simulation process of the discharge propagation along an insulator string is shown in Fig.4.

The discharge process is started with the formation of the first corona. When the streamer is initiated, it starts propagating along the insulator with length L. The streamer has a form of many branches within a conical volume. The filamentary branched channels - streamers, are developed from a common root called stem. The corona zone extends to the coordinate x_s on the discharge axis. It is assumed, that the corona zone is characterized by constant electric field $E_s = 450kV/m$. The total accumulated charge

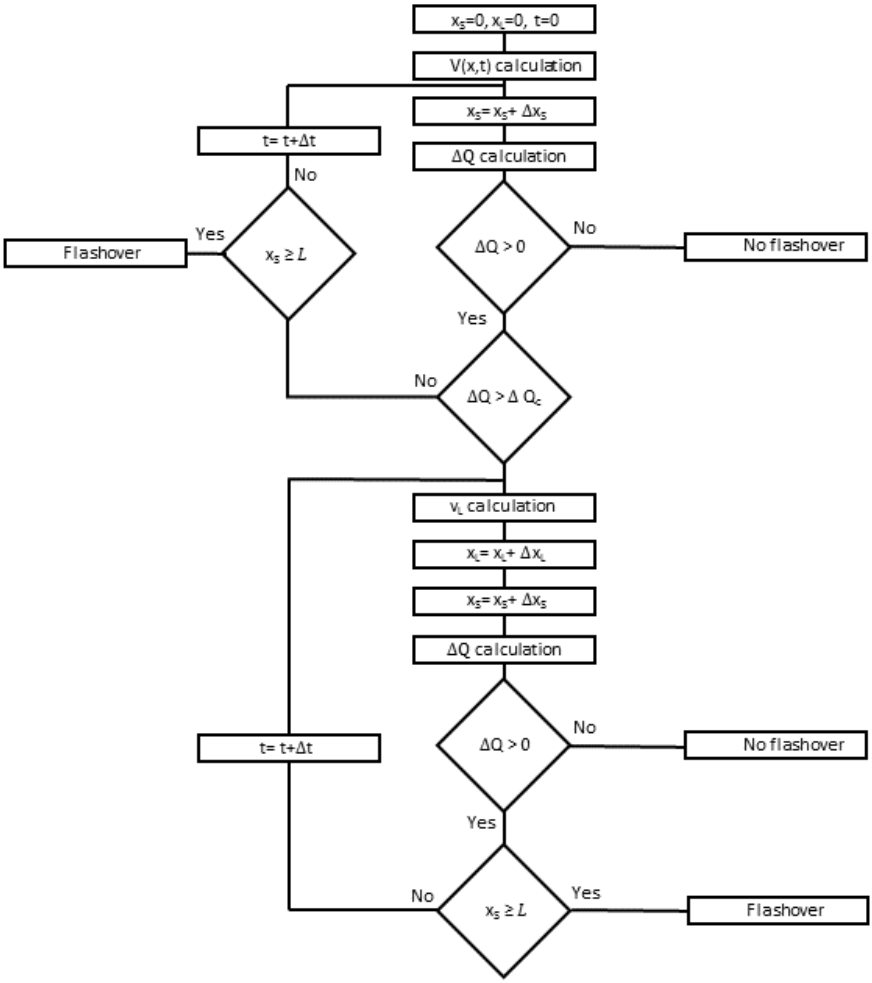

Figure 4: Flow chart of simulation algorithm

in the corona zone is a function of the area between the potential distributions before and after the steamer formation, see Fig. 5.

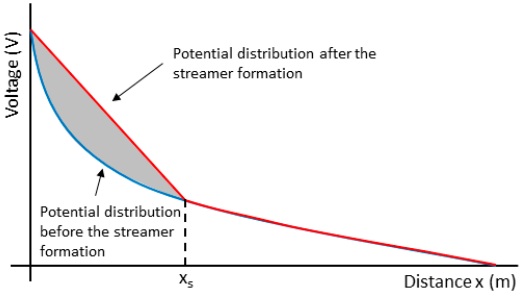

Figure 5: Potential distribution before and after the streamer formation

It is assumed, that the stable propagating leader is initiated when the critical total charge increment $\Delta Q_c = 1\ \mu C$ is reached. The total charge increment is calculated according to equation (4). The leader extension Δx_L is then calculated from the leader velocity, see equation (6). The constant q_l is assumed as the average value 45 $\mu C/m$ and the charge of the streamer zone in front of the leader's head ΔQ is calculated from equation (4). The streamer-leader system step by step propagates along the insulator and in the moment when it across the whole distance L the flashover occurs. If the charge increment during the propagation process is less than zero, the whole process is stopped with the result that no flashover occurs.

3.2 Electric field calculation

The electric field distribution has a crucial role in the discharge propagation process. The electric field distribution is rapidly changing in time when the impulse voltage is applied. Analytical solutions are possible only for simple electrode cases and the more precise numerical calculations like FEM have to be involved. However, FEM requires the exact geometrical description of insulator arrangement and a large amount of computation time. On the other hand, the proposed simulation model needs relatively

fast recalculation of the electric field during the simulation process. The simple and enough accurate solution could be the representation of the insulation string as an equivalent circuit with distributed parameters. Parameters of passive elements are adjusted to approximate the voltage distribution $V(x)$ determined from FEM calculation at the time, when the impulse reach the maximum. Then, the voltage distribution function $V(t, x)$ can be derived from the equivalent circuit equations.
The equivalent circuit of insulator string is shown in Fig. 6.

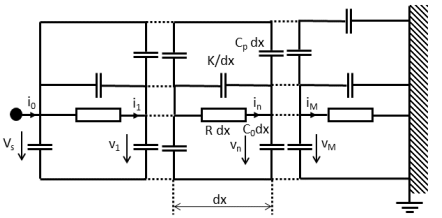

Figure 6: Equivalent circuit of insulator string

The circuit consists of resistor R (Ω/m), insulator to ground capacity C_0 (F/m), insulator to wire capacity C_p (F/m) and capacity of insulator K (Fm). In fact, these parameters are not constant with x coordinate and the linear or exponential function can be used to express this dependency. In some cases, the constant values are assumed to simplify calculations. From the voltage and current relations in an element dx and after some mathematical modifications the final partial differential equation has a form of:

$$\frac{\partial^4 v(t,x)}{\partial x^2 \partial t^2} + \frac{1}{RK}\frac{\partial^3 v(t,x)}{\partial x^2 \partial t} + \frac{C_p}{K}\frac{\partial^2 (v(t,x) - V_s(t))}{\partial^2 t} - \frac{C_0}{K}\frac{\partial^2 v(t,x)}{\partial^2 t} = 0, \tag{11}$$

where $v(t, x)$ is the instantaneous voltage at time t and distance x from the high voltage electrode and $V_S(t)$ instantaneous voltage of the source. The impulse voltage $V_S(t)$ can be described by double exponential model. The equation (12) can be solved by numerical methods only. Assuming the continuous time and

discrete distance x we can make a decomposition into the system of differential equations of first order. Each n-th element is then described by a pair of equations:

$$K\left(\frac{d(v_{n-1}(t)-v_n(t))}{dt}-\frac{d(v_n(t)-v_{n+1}(t))}{dt}\right)+i_n(t)-i_{n+1}(t)$$
$$+C_p\frac{d(V_s(t)-v_n(t))}{dt}-C_0\frac{dv_n(t)}{dt}=0,$$

$$v_{n-1}(t)-v_n(t)-Ri_n(t)=0. \tag{12}$$

Thus, for n elements we get $2n$ equations with the same number of unknown currents and voltages. The resulted voltages and currents in each node are functions of time. The parameters R, K, C_p and C_0 are given by geometrical configuration, insulation material and also by pollution or ice layer on insulator surface. The electrostatic field distribution of suspension glass insulator can be calculated in FEM software to get voltage distribution and approximations of equivalent circuit parameters. The rotationally symmetrical geometry of insulator is supposed, thus the 2D model can be built up. Respecting experimental measurement condition, the high potential is placed on the top of the insulator string, and the ground is connected to the shielding ring placed on the end of insulator string. The voltage distribution is then in opposite direction compare to the case of a real insulator on a tower of overhead line. The rest of the metallic parts has a floating potential. The polluted ice layer can be simulated as a parallel layer copying the insulator surface with given specific conductivity. As can be seen from experimental measurements in the cold room the ice layer and icicles morphology on insulator string may be varied. However, for the higher thicknesses of ice (more than 1.5 cm) the particular insulators are almost fully bridged by icicles. The main assumption, for the FEM geometry of insulator string covered by an ice layer, is that the ice layer bridges all insulator caps by a consistent layer of ice with appropriate thickness. The relative permittivity of the ice layer under switching impulse can be considered equal to the steady state permittivity 76. For the lightning impulse, the relative permittivity decreases to the value

between 3 and 4 [15]. The example of determined electric field distribution of insulator string for dry condition is shown in Fig. 7 and for the polluted ice layer of 3 cm thickness in Fig. 8.

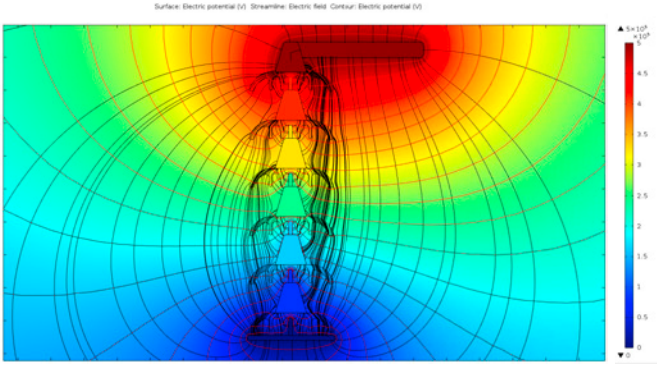

Figure 7: Electric field of suspension insulator string (applied voltage 500 kV)

The voltage distribution along the length of the insulator string for maximal voltage is shown in Fig. 9 and Fig. 10. Cutting lines are in the center of insulator, in the half of insulator radius and the insulator radius.

As can be seen from presented figures, the potential distribution along the insulator string is close to the linear distribution. The reason is, that there are not present any large grounded parts or conductor during the high voltage tests, which could increase the capacity to the ground or capacity to the conductor.

The determined voltage distribution approximation can be used for the simulation of the flashover process. The Fig. 11 shows voltage distributions which are derived from the Fig. 9 and Fig. 10 respecting the resistance of polluted ice layer.

The above described mathematical model for the flashover performance prediction of suspension insulator string was realized in Wolfram Mathematica®. The created mathematical model allows to calculate the streamer-leader propagation process for different shapes of impulse voltages of both polarities. This model can take into consideration an influence of pollution and icing condition.

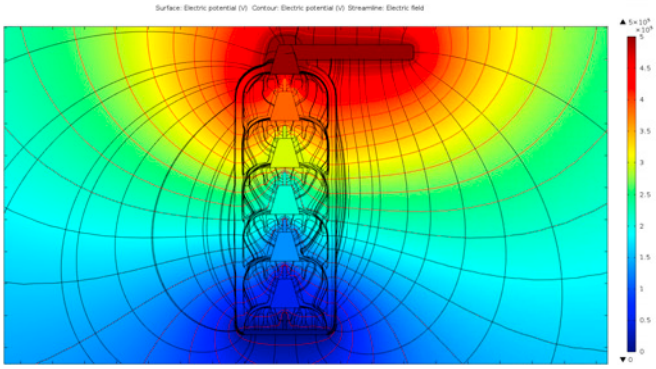

Figure 8: Electric field of suspension insulator string - 3 cm ice layer simulation (applied voltage 500 kV)

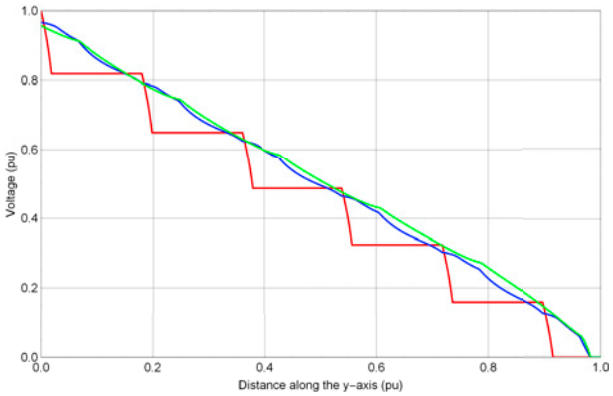

Figure 9: Voltage distribution along the length of the insulator string in the center (red), in the half radius of the insulator (blue) and in the maximal radius of the insulator (green)

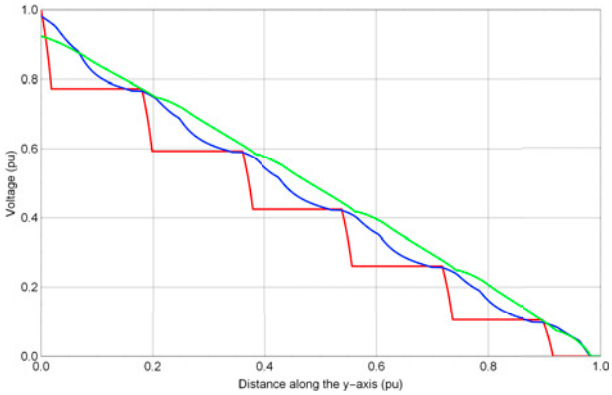

Figure 10: Voltage distribution along the length of the insulator string with 3 cm ice layer in the center (red), in the half radius of the insulator (blue) and in the maximal radius of the insulator (green)

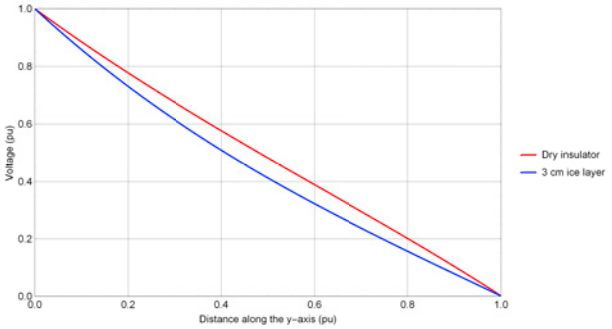

Figure 11: Approximation of voltage distribution along the length of the insulator string

The simulation model can be verified by experimental measurements under the pollution and icing condition.

4 Experimental verification of numerical model

4.1 Experimental setup

Experimental measurements were carried out in the setup according to Fig. 12. The impulse voltage generator (HighVolt IP 40/800L) consists of eight stages and the theoretically reachable peak voltage is 800 kV at 40 kJ of energy. The impulse generator is fully controlled by SGB 1 operator device. The output voltage is measured by damped capacitive impulse voltage divider when its total capacity together with the capacity of high voltage bushing and capacity of a test object creates the load capacity of the impulse generator. The leakage current can be measured by coaxial shunt R_s with the resistivity of 200 $m\Omega$ and connected directly to the ground branch of the circuit. The coaxial shunt is frequency independent up to 1 MHz. The voltage and current waveforms are recorded by 8-bit digital scope with maximal sample rate 1 GSa/s.

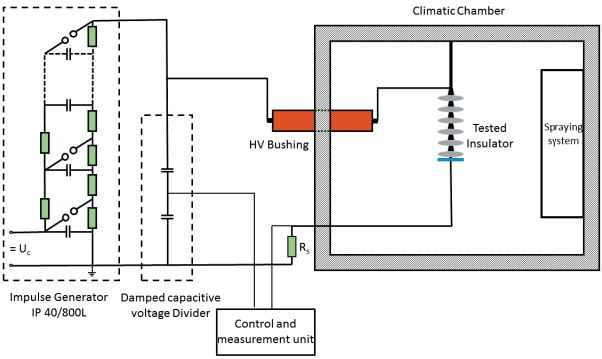

Figure 12: Test circuit for insulator in climatic chamber

The tested insulator string was placed in a vertical climatic room at CIGEL laboratory with dimensions 6 x 6 x 9 m (w x l x h). The climatic room is equipped by spraying system which consists of eight pneumatic nozzles and fans with variable speed control. The temperature inside the chamber can be controlled up to the maximal value of $60\ °C$. The output voltage from the impulse generator is led into the climatic room through the high voltage bushing.
The tested suspension glass insulator string consists of six standard profile insulators of 280 mm in diameter, spacing 147 mm and creepage distance 380 mm, see Fig. 13. The end of the insulator string was equipped by the grading ring to homogenize nonuniform electric field.

Figure 13: Test circuit for insulator in climatic chamber

4.2 Ice formation and the test procedure

The ice layer covering the insulator surface was created from supercooled droplets produced by a spraying system with a uniform airflow obtained from the system of fans. The water conductivity of 80 $\mu S/cm$ were prepared by addition of sodium chloride NaCl to the de-ionized water. The water conductivity was kept constant during all the tests and was verified at the beginning of each test procedure. The insulator was energized by ac operating voltage during the ice accumulation phase. The ice quantity was

determined by measuring the ice thickness increment on monitoring cylinder placed directly at the place of tested insulator, see Fig. 14. The increment of ice thickness with time is shown in Fig. 15.

Figure 14: Monitoring cylinder

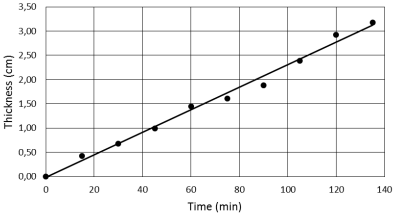

Figure 15: Time dependency of ice thickness on monitoring cylinder

The flashover test was performed according to the melting regime test procedure standardized in [16]. This procedure consists of three consecutive stages. In the first stage, the ice is created at temperature $-12\ ^{\circ}C$ for an appropriate time which is given for required thickness by the graph in Fig.15. After that, the 15 min ice hardening period is performed. During this period, the ac source is reconnected to the impulse generator. Then, the temperature is increased above $0\ ^{\circ}C$ to start the melting process. This stage is confirmed visually as the water film was present at the ice surface. The last stage was the impulse voltage test when the standard up and down method was used to determine the flashover voltage V_{50} and the standard deviation s. The maximum likelihood method for normal distribution was used to evaluate parameters of this voltage test.
The three shapes of impulses were generated to investigate the flashover performance of insulator covered by an ice layer:

- Lightning impulse (LI) with front time 1.2 μs and half time 50 μs
- Switching impulse (SW-1) with front time 100 μs and half time 2500 μs
- Switching impulse (SW-2) with front time 250 μs and half time 2500 μs

These impulses represent different frequency content and transients in electrical power systems. The example of iced insulator after the ice creation stage is shown in Fig. 16. The path of the arc during the impulse high voltage test can be traced on Fig. 16.

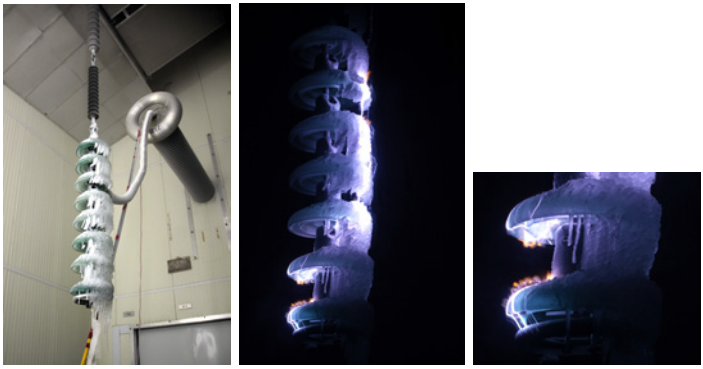

Figure 16: Tested insulator string after the ice accumulation stage (left), the arc trajectory (middle) and the detail of the arc trajectory for two bottom insulators (right)

4.3 Experimental results

4.4 Influence of ice thickness on the insulator flashover voltage

The flashover voltage for impulse voltages and ice layer thickness in the range up to approximately 3 cm are shown in Fig. 17, Fig. 18 and Fig. 19. Errors bars represents the determined standard deviation of flashover voltage extended by coefficient k=2

to reach 98 % probability. This error doesn't exceed the value of 16 kV for all measured values.

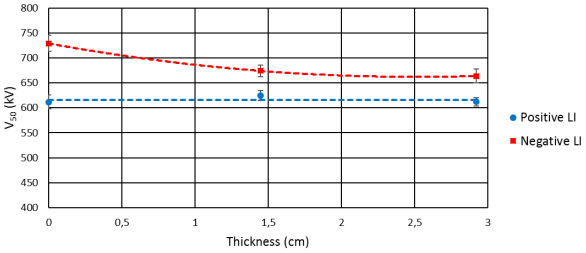

Figure 17: Flashover voltage V_{50} for lightning impulse (1.2/50 μs) of both polarities as ice layer thickness dependency

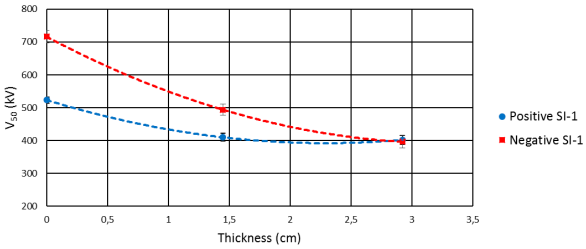

Figure 18: Flashover voltage V_{50} for switching impulse (100/2500 μs) of both polarities as ice layer thickness dependency

As can be seen from determined flashover voltages for the clean insulator the values have decreasing tendency with increasing front duration of the impulse. This effect was described by many tests in the past for various arrangements [17] and it may be considered as a proof of results validity.

4.5 Simulation results and verification

As the experimental measurements show, the switching impulses of positive polarity are more critical regarding flashover performance of suspension insulator under the polluted and ice

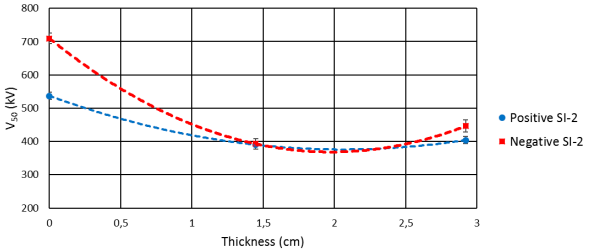

Figure 19: Flashover voltage V_{50} for switching impulse (250/2500 μs) of both polarities as ice layer thickness dependency

conditions. Thus, the simulation model was validated for such conditions and results were compared with determined data from laboratory experiments. The comparison of flashover voltage V_{50} for dry and two thicknesses of ice layer are shown in Fig. 20, comparison of voltage - time characteristic for dry insulator on Fig. 21 and the comparison of voltage - time characteristic for ice layer of 2.92 cm.

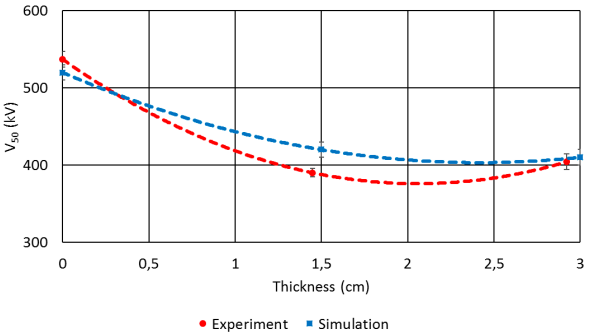

Figure 20: Flashover voltage V_{50} for switching impulse (250/2500 μs) as ice layer thickness dependency - comparison of calculated and experimental data

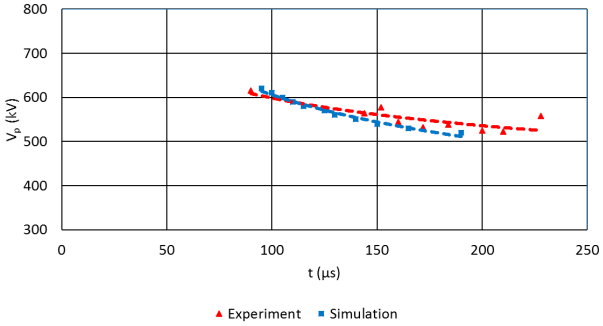

Figure 21: Voltage - time characteristic for switching impulse (250/2500 μs) fro dry insulator - comparison of calculated and experimental data

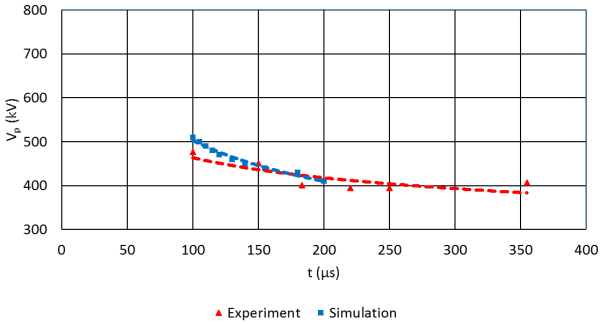

Figure 22: Voltage - time characteristic for switching impulse (250/2500 μs) for 2.92 cm ice layer - comparison of calculated and experimental data

5 Conclusion

Experimental measurements performed on the suspension string of cap and pin glass insulator in Industrial Research Chair on Atmospheric Icing of Power Network Equipment (CIGELE), University of Quebec at Chicoutimi show that the presence of ice layer has significant influence to the flashover performance and

volt-time characteristics of suspension insulators when they are exposed to the transient overvoltage with different front times. In case of switching impulses, the flashover voltage reduction reached the value of 25 % for the positive polarity, and 44 % for the negative polarity. The experimental results were further used for the validation of mathematical model simulating physical processes during flashover when various impulse voltages are applied. The algorithm of the dynamic simulation model was fully described on the base of physical background of streamer-leader propagation for a long air gap study. The simulation model allow to calculate flashover voltages for different shapes of test impulse voltages and to take into consideration influence of pollution and icing conditions. The presented comparison with experimental measurements confirms that the proposed simulation model can give reasonable accurate values of flashover voltages which are sufficient for high voltage test engineers.

References

[1] I Gallimberti. A computer model for streamer propagation. *Journal of Physics D: Applied Physics*, 5(12):2179, 1972.

[2] G. Baldo, I Gallimberti, H. N. Garcia, B. Hutzler, J. Jouaire, and M. F. Simon. Breakdown phenomena of long gaps under switching impulse conditions influence of distance and voltage level. *Power Apparatus and Systems, IEEE Transactions on*, 94(4):1131–1140, July 1975.

[3] Les Reanrdieres Group. Double impulse tests of long airgaps. part 2: Leader decay and reactivation. *Physical Science, Measurement and Instrumentation, Management and Education - Reviews, IEE Proceedings A*, 133(7):410–437, October 1986.

[4] Les Reanrdieres Group. Double impulse tests of long airgaps. part 3: Voltage front perturbation effects. *Physical Science, Measurement and Instrumentation, Management and Education - Reviews, IEE Proceedings A*, 133(7):438–468, October 1986.

[5] Les Reanrdieres Group. Double impulse tests of long airgaps. part 4: Effects of pre-existing space charge on positive discharge development. *Physical Science, Measurement and Instrumentation, Management and Education - Reviews, IEE Proceedings A*, 133(7):469–483, October 1986.

[6] Les Reanrdieres Group. Double impulse tests of long airgaps. part 1: Engineering problems and physical processes: the basis of recent tests. *Physical Science, Measurement and Instrumentation, Management and Education - Reviews, IEE Proceedings A*, 133(7):395–409, October 1986.

[7] N Goelian, P Lalande, A Bondiou-Clergerie, G L Bacchiega, A Gazzani, and I Gallimberti. A simplified model for the simulation of positive-spark development in long air gaps. *Journal of Physics D: Applied Physics*, 30(17):2441, 1997.

[8] A Bondiou and I Gallimberti. Theoretical modelling of the development of the positive spark in long gaps. *Journal of Physics D: Applied Physics*, 27(6):1252, 1994.

[9] I. Gallimberti. The mechanism of long spark formation. *J. Phys. Coll.*, C7(40):193–250, 1979.

[10] I Gallimberti, G Bacchiega, Anne Bondiou-Clergerie, and Philippe Lalande. Fundamental processes in long air gap discharges. 3:1335–1359, 2002.

[11] F. A M Rizk. A model for switching impulse leader inception and breakdown of long air-gaps. *Power Delivery, IEEE Transactions on*, 4(1):596–606, Jan 1989.

[12] Farouk A.M. Rizk. Switching impulse strength of air insulation: leader inception criterion. *Power Delivery, IEEE Transactions on*, 4(4):2187–2195, Oct 1989.

[13] Farouk A.M. Rizk. Critical switching impulse strength of long air gaps: modelling of air density effects. *Power Delivery, IEEE Transactions on*, 7(3):1507–1515, Jul 1992.

[14] E.M. Bazelyan and Y.P. Raizer. *Spark Discharge*. Taylor & Francis, 1997.

[15] T. Guerrero, M. Farzaneh, and J. Zhang. Impulse voltage performance of ice-covered post insulators. In *Annual Report Conference on Electrical Insulation and Dielectric Phenomena*, pages 341–344, 2005.

[16] *IEEE Std 1783-2009 Guide for Test Methods and Procedures to Evaluate the Electrical Performance of Insulators in Freezing Conditions*, IEEE Standard, 2009.

[17] J. Kuffel, E. Kuffel, and W.S. Zaengl. *High Voltage Engineering Fundamentals*. Elsevier Science, 2000.

6 Ing. Radek Prochazka, Ph.D.

Personal Information

- Date of birth: July 12, 1976
- Place of birth: Most, Czech Republic
- Nationality: Czech
- E-mail: xprocha3@fel.cvut.cz

Education

- **2007 - Ph.D. Electrical Power Engineering**, Czech Technical University in Prague, Faculty of Electrical Engineering, Prague, Czech Republic
- **2002 - M.Sc.-equivalent in Electrical Power Engineering**, Czech Technical University in Prague, Faculty of Electrical Engineering, Prague, Czech Republic

Employment

- **2005 - Present** Assistant professor, Czech Technical University in Prague, Faculty of Electrical Engineering
- **2014 - 2014**, Postdoctoral fellow, Industrial Chair on Atmospheric Icing of Power Network Equipment (CIGELE), University of Quebec in Chicoutimi, Canada
- **2002–2005** Technician, Researcher, Czech Technical University in Prague, Faculty of Elctrical Engineering
- **2001–2002** Technician, Strategy and Trade Department, Czech Transmission System Operator, Prague

Teaching

- High Voltage Engineering - lecturer
- Power Engineering I - lecturer

- High voltage testing - lecturer
- Master and bachelor thesis suprevisor

Citation and Impact

- H-index: 2
- Web of Science citations: 18

Selected publication

1. Procházka, R. - Hlaváček, J. - Draxler, K.: Magnetic Circuit of a High-voltage Transformer up to 10 kHz. IEEE Transactions on Magnetics. 2015, vol. 51, no. 1, art. no. 7029203, ISSN 0018-9464.

2. El-Zohri, EH - Ziedan, H. - Procházka, R.: A new proposed dynamic arc model for flashover performance of a non-uniform polluted insulator string under HVAC stress. Electric Power Systems Research. 2015, vol. 119, p. 278-286. ISSN 0378-7796.

3. Procházka, R. - Hlaváček, J. - Draxler, K.: Impulse Current Transformer With a Nanocrystalline Core. IEEE Transactions on Magnetics. 2013, vol. 49, no. 1, p. 77-80. ISSN 0018-9464.

4. Draxler, K. - Styblíková, R. - Hlaváček, J. - Procházka, R.: Calibration of Rogowski Coils with an Integrator at High Currents. IEEE Transactions on Instrumentation and Measurement. 2011, vol. 60, no. 7, p. 2434-2438. ISSN 0018-9456.

5. Prochazka, R. - Farzaneh, M. - Tlusty, J. - Sklenicka, V.: Laboratory study of flashover performance of polluted and ice-covered insulators exposed to impulse overvoltage.19th International Symposium on High Voltage Engineering , Pilsen, 2015 ,ISBN 978-80-261-0477-3

6. Procházka, R. - Draxler, K. - Hlaváček, J. - Styblíková, R.: Precise 10 and 20 kV DC/AC Resistive Divider. In I2MTC - 2013 IEEE International Instrumentation and Measurement Technology Conference. Piscataway: IEEE, 2013, p. 774-777. ISBN 978-1-4673-4622-1

7. Lachi, S. - Prochazka, R. - Tlusty, J. - Lilien, J., L.: Overhead line partial discharges detection.19th International Symposium on High Voltage Engineering , Pilsen, 2015 ,ISBN 978-80-261-0477-3

8. Sláma, J. - Píchal, J. - Procházka, R.: Plasma Flow in Different Gliding Discharge Reactor Configurations. Acta Technica CSAV. 2011, vol. 56, no. supplement, p. T397-T403. ISSN 0001-7043.

9. Draxler, K. - Procházka, R. - Michal Ulvr, M. - Renata Styblíková, R.: Measuring the Remanent Factor of TPY Class Transformers. Journal of Electrical Engineering. 2012, vol. 63, no. 7s, p. 71-74. ISSN 1335-3632.

10. Ziedan, H. - Tlustý, J. - Mizuno, A. - Sayed, A. - Ahmed, A. - Prochazka, R..: Finite elements, Deutsch's assumption, corona onset voltage, corona space charge, wire-duct precipitators. International Journal of Plasma Environmental Science & Technology. 2011, vol. 5, no. 1, p. 68-79. ISSN 1881-8692.